

Cellular uptake and subcellular distribution of chlorin e6 as functions of pH and interactions with membranes and lipoproteins

Halina Mojzisova, Stéphanie Bonneau, Christine Vever-Bizet, Daniel Brault *

Laboratoire de Biophysique Moléculaire Cellulaire et Tissulaire (BIOMOCETI), CNRS UMR 7033, Université Pierre et Marie Curie, Paris, France

Received 9 May 2007; received in revised form 5 July 2007; accepted 9 July 2007

Available online 13 July 2007

Abstract

The uptake and more importantly the subcellular distribution of photosensitizers are major determinants of their efficacy. In this paper, the cellular internalization of chlorin e6 (Ce6), a photosensitizer bearing three carboxylic chains, is considered with emphasis on pH effects. Small unilamellar vesicles are used as models to investigate the dynamics of interactions of Ce6 with membranes. The entrance and exit steps from the outer lipid hemileaflet are very fast (~ms). A slow transfer of Ce6 through the membrane was observed only for thin bilayers made of dimyristoleoyl-phosphatidylcholine. Ce6 did not permeate through bilayers consisting of longer phospholipids more representative of biological membranes. These results along with previous data on the interactions of Ce6 with low-density lipoproteins (LDL) are correlated with cellular studies. After 15 min incubation of HS68 human fibroblasts with Ce6, fluorescence microscopy revealed labeling of the plasma membrane and cytosolic vesicles different from lysosomes. When vectorized by LDL, Ce6 was mainly localized in lysosomes but absent from the plasma membrane. Internalization of LDL bound photosensitizer via ApoB/E receptor mediated pathway was demonstrated by overexpression experiments. A pH decrease from 7.4 to 6.9 did not affect the intracellular distribution of Ce6, but significantly increased its overall cellular uptake.

© 2007 Elsevier B.V. All rights reserved.

Keywords: Photosensitizer; Cellular uptake; Subcellular localization; pH; Lipoprotein; Model membranes

1. Introduction

Photodynamic therapy (PDT), a promising treatment of several oncologic and ophthalmologic diseases, is based on light induced excitation of photosensitizing molecules, producing transient toxic species such as singlet oxygen and free radicals [1,2]. Since the lifetime of these species is extremely short, they diffuse poorly in a biological environment and the photoinduced damages affect primarily the cell structures labeled with the drug. Hence, the subcellular localization of the photosensitizers is a major factor governing the extension of the photoinduced cell damage as well as the mechanism of the consequent cell death [3,4].

* Corresponding author. Laboratoire de Biophysique Moléculaire Cellulaire et Tissulaire (BIOMOCETI) CNRS UMR 7033, Genopole Campus 1, 5 rue Henri Desbruères, 91030 EVRY cedex, France. Fax: +33 1 69 87 43 60.

E-mail address: dbrault@ccr.jussieu.fr (D. Brault).

Because of their enhanced absorption of light in the “therapeutic” window (600–800 nm), chlorins are attractive photosensitizing agents for therapeutic applications. In this series, chlorin e6 (Ce6) and its derivatives display promising properties [5,6]. Chlorin e6 is an asymmetric molecule bearing three ionizable carboxylic groups. The neutralization of the charge of these groups at slightly acidic pH increases the Ce6 lipophilicity. As a consequence, its interactions with biological structures such as plasma proteins and lipid membranes are modified. In a previous study, we have shown that the Ce6 fraction bound to lipid membranes and low density lipoproteins (LDL) increases whereas the one bound to HSA decreases when the pH changes from 7.4 to 6.5 [7]. Since the pH of tumor stroma is decreased compared to that of normal tissue [8,9], the enhanced lipophilicity might favor the cellular uptake of Ce6 by neoplastic cells and thus increase the selectivity of the photosensitizer for tumors.

The cellular internalization pathway and subcellular localization are related to the structural and physico-chemical characteristics of

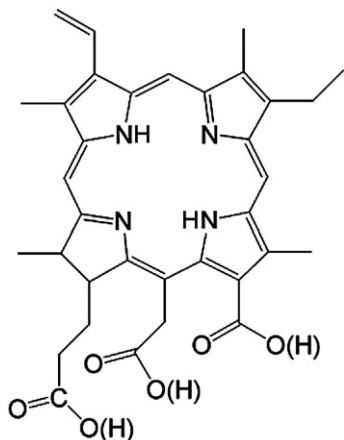


Fig. 1. Structure of Chlorin e6 (Ce6).

the photosensitizer. The drug can incorporate into cells either by passive diffusion through the plasma membrane, or by following the endocytosis pathway. The balance between these two mechanisms is determined by the interactions of the photosensitizer with cell membranes and blood carriers, especially with LDL. As a matter of fact, LDL have been proposed by several authors to be carriers of hydrophobic photosensitizers [10–13]. Moreover, the increased cholesterol need of proliferating tissues induces the over-expression of apo B/E receptors on the cell surface [14,15]. Thus, the cellular incorporation of lipoprotein bound sensitizers via LDL specific endocytosis may be one of the mechanisms leading to the preferential retention of the photosensitizers by tumors.

The aim of the present work is to evaluate the effect of decreased pH on the cellular internalization and the mechanism of cellular entrance of Ce6. Firstly, models of lipid membranes are used to study the effect of pH on the kinetics of the interactions between Ce6 and the lipid bilayer. In the second part, these physico-chemical parameters are correlated with the cellular internalization and the subcellular localization of free and LDL-bound Ce6.

2. Materials and methods

2.1. Chemicals

Chlorin e6 (Fig. 1) was purchased from Porphyrin Products, Logan (UT, USA). A stock solution (1 mM) was prepared in 20 mM Na_2HPO_4 . The experimental Ce6 solutions were diluted in PBS (20 mM Na_2HPO_4 , 20 mM KH_2PO_4 , 150 mM NaCl, pH=7.4) and handled in the dark to avoid any photobleaching.

Human low-density lipoproteins (LDL) were purchased from Calbiochem (San Diego, CA, USA). They were conditioned at a concentration of 9.52 mg/ml (protein content) in 150 mM NaCl, pH 7.4 aqueous solution with 0.01% EDTA.

Chloroform (MERCK, Darmstadt, Germany) was of spectroscopic grade quality.

2.2. Liposome preparation

Di-oleoyl-*sn*-phosphatidylcholine (DOPC, C18:1) and Dimyristoleoyl-*sn*-phosphatidylcholine (DMoPC, C14:1) were purchased from Avanti Polar Lipids (Alabaster, AL, USA). Lipids were dissolved in chloroform and the solution was taken to dryness. The lipid film obtained was rehydrated by PBS and vortexed for several minutes. The liposome suspension was extruded 10 times through a stack of two polycarbonate membrane filters (Poretics, Livermore, Ca, USA) with a pore size of 100 nm, by using an extruder device (Lipex, Biomembranes, Vancouver, Canada).

2.3. Kinetics measurements

Fast kinetics measurements were performed at either 20 °C or 37 °C by using a stopped flow apparatus (Applied Photophysics, Leatherhead, UK) with a mixing time of 1.2 ms. The excitation was provided by a 150-W Xenon lamp. The slits of the excitation monochromator were set to give a bandwidth of 4.65 nm. The emitted light was collected through a 665-nm cut-off filter (Oriol, Palaiseau, France) that transmits red light. The wavelength of 665 nm corresponds to 50% transmittance. As shown by preliminary experiments, the excitation wavelength yielding the best signal was 411 nm. The signal was processed by a RISC workstation (Acorn Computers, Cambridge, UK). The data analysis was performed by using the Kaleidagraph® software (Synergie Software, PA, USA).

Slow kinetics measurements were performed with an Aminco Bowman Series 2 spectrofluorimeter (Edison, NJ, USA). The excitation wavelength was set to 408 nm and the time trace of the fluorescence emission at 670 nm was recorded. The emission wavelength (670 nm) was slightly red-shifted compared to the emission maximum of Ce6 (668 nm) in order to detect kinetics signal with maximal amplitude. The same set of wavelength was used in our previous paper [7] to analyze equilibrium data.

2.4. Cell culture experiments

Cells from the human fibroblast cell line HS68 were grown at 37 °C (5% CO_2 atmosphere) in DMEM (Dulbecco's Minimum Eagle Medium) supplemented with 10% foetal calf serum (FCS) and 100 U/mol Penicillin/Streptomycin. The cellular experiments were performed at pH 7.4 and 6.9. The acidic pH value is higher than 6.5 used in kinetics experiments because of fragility of the cell culture. Spectroscopic studies have shown that the pH decrease to 6.9 is sufficient to establish the Ce6 protonation equilibria shift towards the neutralization of the carboxyl groups.

2.4.1. Quantification of Ce6 uptake

HS68 cells were seeded in Petri dishes and collected at confluence for the experiments. The cells were washed with HBSS (Hank's balanced salt solution) and incubated for 15 min with HBSS containing 5×10^{-7} M Ce6 alone or preloaded in 1×10^{-7} M LDL. Taking into account the lipoprotein concentration and LDL binding constant value $K_{\text{LDL}} = 6.9 \times 10^7$ M [7], more than 85% of Ce6 molecules were bound to LDL in these conditions. After incubation, the cells were washed

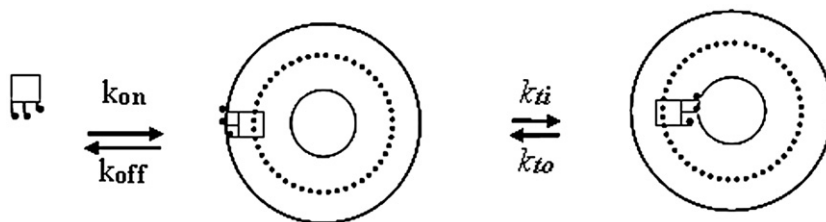


Fig. 2. Scheme of Ce6–liposome interactions.

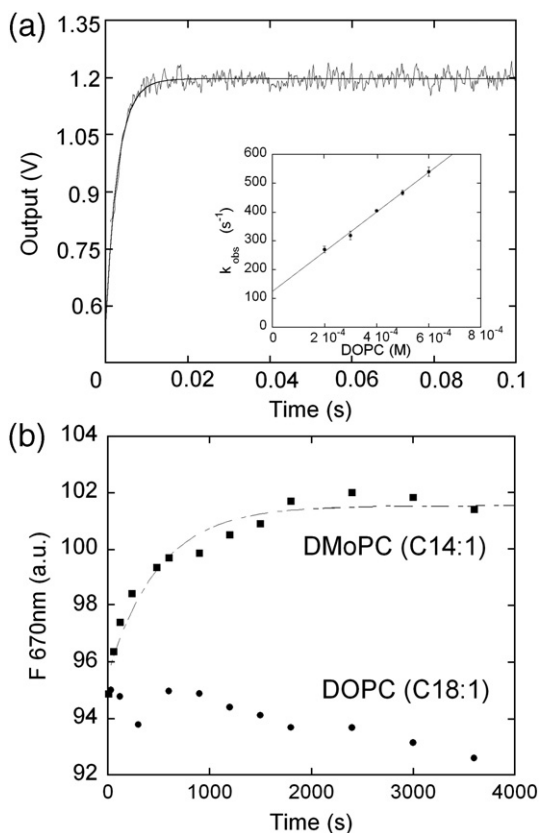


Fig. 3. Kinetics of the Ce6 interactions with the lipid vesicles at pH=7.4. (a): The first phase of the Ce6 incorporation. The fluorescence intensity changes upon mixing DOPC liposomes (1×10^{-4} M) with Ce6 (5×10^{-7} M), $t=20$ °C. (a) inset: Fast phase rate constant k_1 versus DOPC concentration. $[Ce6]=5 \times 10^{-7}$ M. The slope and the intercept at the origin of the linear fit give the values of $k_{on}^{obs}=6.88 \times 10^5$ M $^{-1}$ s $^{-1}$ and $k_{off}^{obs}=125$ s $^{-1}$. (b): The slow phase of the Ce6 interaction with the lipid vesicles. The fluorescence intensity changes upon mixing DOPC and DMOPC liposomes (1×10^{-4} M) with Ce6 (5×10^{-7} M) recorded by using the spectrofluorimeter. The temperature was increased up to 37 °C. Excitation wavelength was set at 410 nm, the fluorescence intensity was measured at 670 nm, where the differences between the fluorescence of Ce6 in aqueous and lipid environment are the most pronounced. The experimental data were fitted by a monoexponential equation giving the rate constant value $k_2=(2.0 \pm 0.3) \times 10^{-3}$ s $^{-1}$.

twice and scraped in 900 μ l of bidistilled water leading to cell lysis. A solution of 3% Triton X-100 (100 μ l) was added to the suspension in order to disrupt the membranes. The fluorescence spectra were measured and compared to calibration curves made with known photosensitizer concentrations in 0.3% Triton X-100 solution. The protein content was determined by the Lowry's method [16]. All experiments were performed in triplicate and the mean values of Ce6 concentration per gram of protein (\pm standard deviation) were calculated.

2.4.2. LDL bound Ce6 receptor mediated uptake

In order to enhance the expression of LDL receptors on the cell surface, the HS68 fibroblasts were incubated during 48 h with DMEM medium supplemented with 2% Ultrosor G [17]. After incubation, the cellular uptake of Ce6 free or associated to LDL was assessed. In parallel, experiments were carried out with cells pre-incubated with DMEM supplemented with 10% FCS. For each type of experiments (Ce6 free or associated to LDL), the mean value for three independent measurements was determined and the uptake was independently normalized to the "non over expressed" samples.

2.4.3. Microscopy experiments and subcellular localization

HS68 cells were seeded on a 0.17-mm thick cover glass 24 h before the experiment. The cells were washed twice with HBSS and incubated for 30 min

with 200 nM LysoTracker[®] green. Then, the cells were incubated for 15 min with HBSS containing 5×10^{-7} M Ce6, alone or preloaded in 1×10^{-7} M LDL.

Ce6 was excited through a bandpass filter 330–380 nm and the red fluorescence emission of the samples was collected through a 645 \pm 75 nm, Omega bandpass filter. For LysoTracker[®] excitation a bandpass filter (484 nm) and a dichroic mirror at 400 nm were used. The LysoTracker[®] fluorescence signal was collected through a bandpass filter (535 \pm 45 nm, Omega). The use of different excitation and emission filters allowed a good separation of the Ce6 red emission from the green emission of LysoTracker[®]. The autofluorescence of controls containing LDL alone or pure HBSS was significantly lower compared to the Ce6 and Lyso Tracker[®] signals. The microscopy equipment has been described elsewhere [18].

3. Results

3.1. Interactions of chlorin e6 with lipid membranes

In the first part of this study, phosphatidylcholine unilamellar vesicles were used as a simple model of the lipid phase of biological membranes. To examine the distribution of Ce6 between the outer and inner membrane layers, our study was

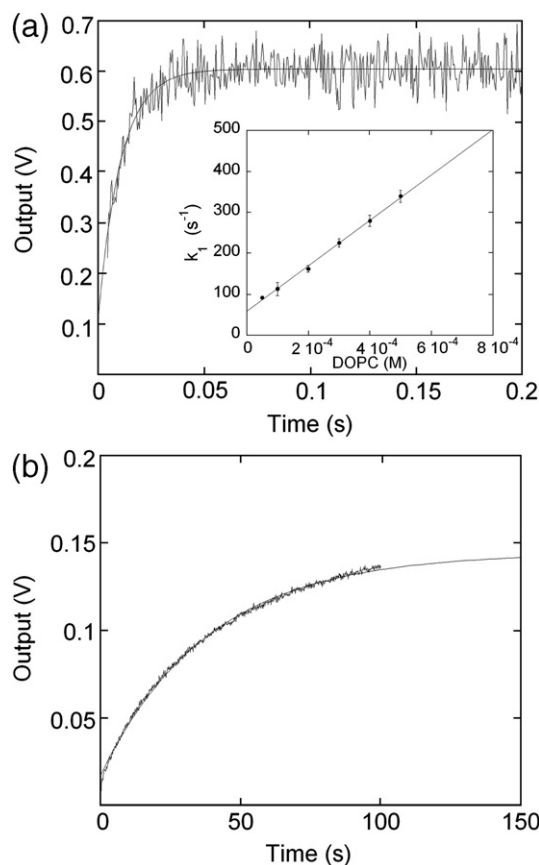


Fig. 4. Kinetics of the Ce6 interactions with the lipid vesicles at pH=6.5. (a): The first phase of the Ce6 incorporation: the fluorescence intensity changes upon mixing DOPC liposomes (1×10^{-4} M) with Ce6 (5×10^{-7} M), $t=20$ °C. (a) Inset: Fast phase rate constant versus DOPC concentration, $[Ce6]=5 \times 10^{-7}$ M. The slope and the intercept at the origin of the linear fit give the values of $k_{on}^{obs}=5.6 \times 10^5$ M $^{-1}$ s $^{-1}$ and $k_{off}^{obs}=58$ s $^{-1}$. (b) Slow phase of the Ce6 interaction with lipid vesicles at pH 6.5. The fluorescence intensity changes upon mixing Ce6 (5×10^{-7} M) and DMOPC liposomes (1×10^{-4} M). Excitation wavelength was set at 411 nm. The experimental data were fitted by a monoexponential equation giving $k_2=(26.3 \pm 0.1) \times 10^{-3}$ s $^{-1}$, $t=37$ °C.

based on the theoretical two-stage kinetics model developed by Kuzelova et al. [19]. This model applies to amphiphilic molecules such as Ce6 bearing polar side chains on one side of the pyrrole macrocycle. Upon mixing with vesicles, a first phase, characterized by a rate constant k_1 , corresponds to the reversible incorporation of the photosensitizer into the outer leaflet of the membrane as shown in Fig. 2. This phase is detected by the fluorescence changes associated to the transfer of the molecule from an aqueous to a lipid environment. Then, the molecules localized in the outer leaflet can flip to the inner leaflet with a rate constant k_2 . Consequently, the outer leaflet is available to incorporate other molecules yielding again fluorescence changes. Provided that $k_1 > k_2$, a two step process is observed and can be fitted by a biexponential. The experiments with Ce6 were carried out at pH 7.4 and 6.5 in order to determine the effect of acidification on the speed of membrane crossing. The pH scale was chosen to be sufficiently large to insure at least the partial protonation of the carboxyl groups.

Ce6 and vesicles were mixed in the stopped-flow apparatus, with the excitation wavelength set at 411 nm. The Ce6 concentration was kept at 5×10^{-7} M and the DOPC concentration varied in the range $1\text{--}5 \times 10^{-4}$ M after mixing. The DOPC to Ce6 molar ratio was at least 200. Due to this excess of DOPC, the first phase of the interaction was considered to obey pseudo-first order conditions. The fluorescence signal was fitted by a monoexponential function giving the pseudo first-order rate constants k_1 . This constant was found to linearly depend on the vesicle concentration. The rate constants for the entrance and exit steps of Ce6 from the outer layer were derived from this linear fit according to the equation:

$$k_1 = k_{\text{on}}^{\text{obs}} \times [\text{DOPC}] + k_{\text{off}}^{\text{obs}} \quad (1)$$

Figs. 3 and 4 show the fluorescence signal of the first phase (a) and the influence of the vesicle concentration on the rate constant k_1 (inset) leading to $k_{\text{on}}^{\text{obs}} = (6.88 \pm 0.28) \times 10^5 \text{ M}^{-1} \text{ s}^{-1}$ and $k_{\text{off}}^{\text{obs}} = 125 \pm 12 \text{ s}^{-1}$ at pH 7.4. At pH 6.5, we obtained $k_{\text{on}}^{\text{obs}} =$

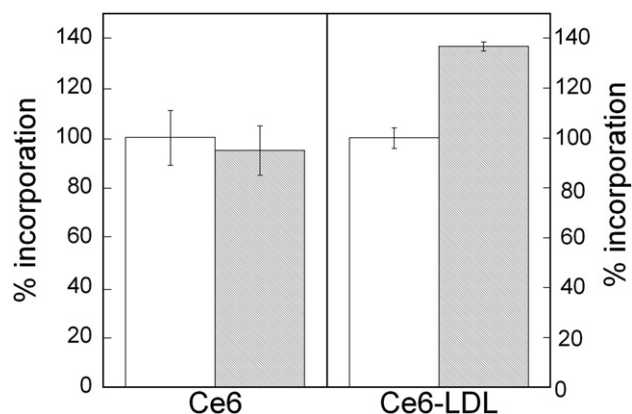


Fig. 5. Effects of LDL receptor expression on the uptake of LDL bound Ce6 by HS68 fibroblasts. Cells were incubated for 48 h either in DMEM medium supplemented with 10% FCS (white) or in DMEM medium supplemented with 2% Ultrosor G (grey). Ce6 uptake by the cells was assessed by fluorescence intensity measurement at 668 nm. The uptake of non-overexpressed cells was normalized to 100% independently for every experiment (Ce6 free or Ce6-LDL).

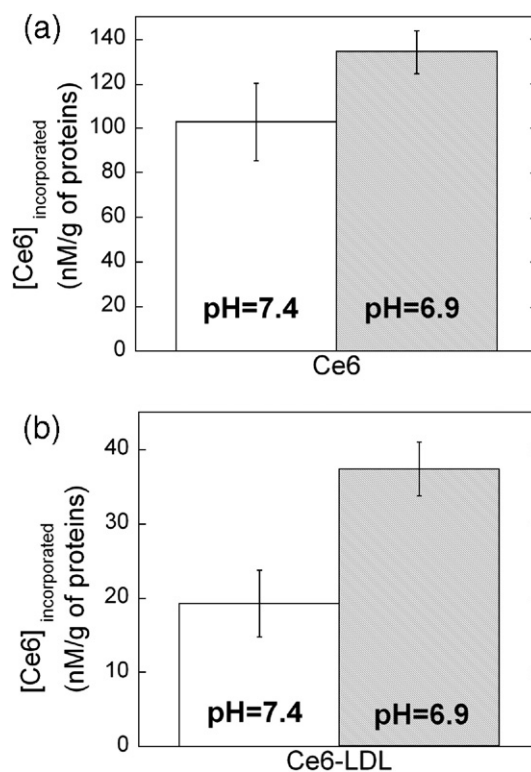


Fig. 6. Uptake of Ce6 by HS68 fibroblasts at pH 7.4 (left) and 6.9 (right) (a) Ce6 free (5×10^{-7} M) (b) Ce6 bound to the LDL (1×10^{-7} M).

$(5.56 \pm 0.12) \times 10^5 \text{ M}^{-1} \text{ s}^{-1}$ and $k_{\text{off}}^{\text{obs}} = 58 \pm 4 \text{ s}^{-1}$. A second phase was not detectable either on the stopped flow apparatus or by using the Aminco spectrofluorimeter in kinetics mode for long records (see below). This means that either the flip-flop between the two hemileaflets was too slow to be observed or too fast to be distinguished from the first phase. In order to check the first hypothesis, conditions that facilitate the flip-flop were chosen. The temperature was increased up to 37°C and the vesicles were made with DMOPC (C14:1), a phospholipid with shorter chains. As discussed below, both conditions should favor the flip-flop significantly. Also, a lower pH leading to the neutralization of the Ce6 carboxylic chains is expected to accelerate the flip-flop. Upon mixing Ce6 with DMOPC vesicles at pH 7.4, very slow changes of fluorescence were recorded. Fig. 3b shows the increase of the fluorescence intensity at 670 nm, corresponding to the fluorescence emitted by Ce6 incorporated in the membrane. The rate constant value calculated for DMOPC was $k_2 = (2.0 \pm 0.3) \times 10^{-3} \text{ s}^{-1}$. The small fluorescence decrease detected with DOPC vesicles are more likely due to the Ce6 photobleaching. Fig. 4b shows the evolution of the fluorescence signal at pH 6.5 using DMOPC vesicles. The curve was fitted by a monoexponential function leading to $k_2 = (26.3 \pm 0.1) \times 10^{-3} \text{ s}^{-1}$. The second phase remained absent with DOPC vesicles.

3.2. Cellular experiments

3.2.1. Cellular uptake

To examine the cellular uptake of Ce6, the HS68 human fibroblasts were incubated in the same conditions in presence of

either free Ce6 or Ce6 associated to LDL. After incubation, the cells were lysed and the concentration of internalized Ce6 was determined by fluorescence and normalized to the protein content of the samples. In order to enhance the expression of the LDL receptors, the cells were incubated in a medium free of lipoproteins [17,20]. A 48-h preincubation in this medium resulted in 37% enhancement of cellular uptake of LDL-bound Ce6, while there was no effect for free Ce6 (Fig. 5). These results confirm the role of the LDL receptor mediated internalization pathway.

The drug uptake was determined at pH 7.4 and 6.9. Fig. 6 represents the amounts of Ce6 incorporated by the cells at pH 7.4. Ce6 is internalized either free or when preloaded to LDL. However, the concentration of intracellular Ce6 is approximately 5 times lower, when Ce6 is bound to LDL compared to free Ce6. The effect of pH is presented in Fig. 6. The acidification increases the uptake of Ce6 either when it is free in solution or when it is vectorized by LDL. The ratio of the concentration of Ce6 incorporated at pH 7.4 to that at 6.9 is approximately 1.3 for the free and 1.9 for the LDL-bound molecule.

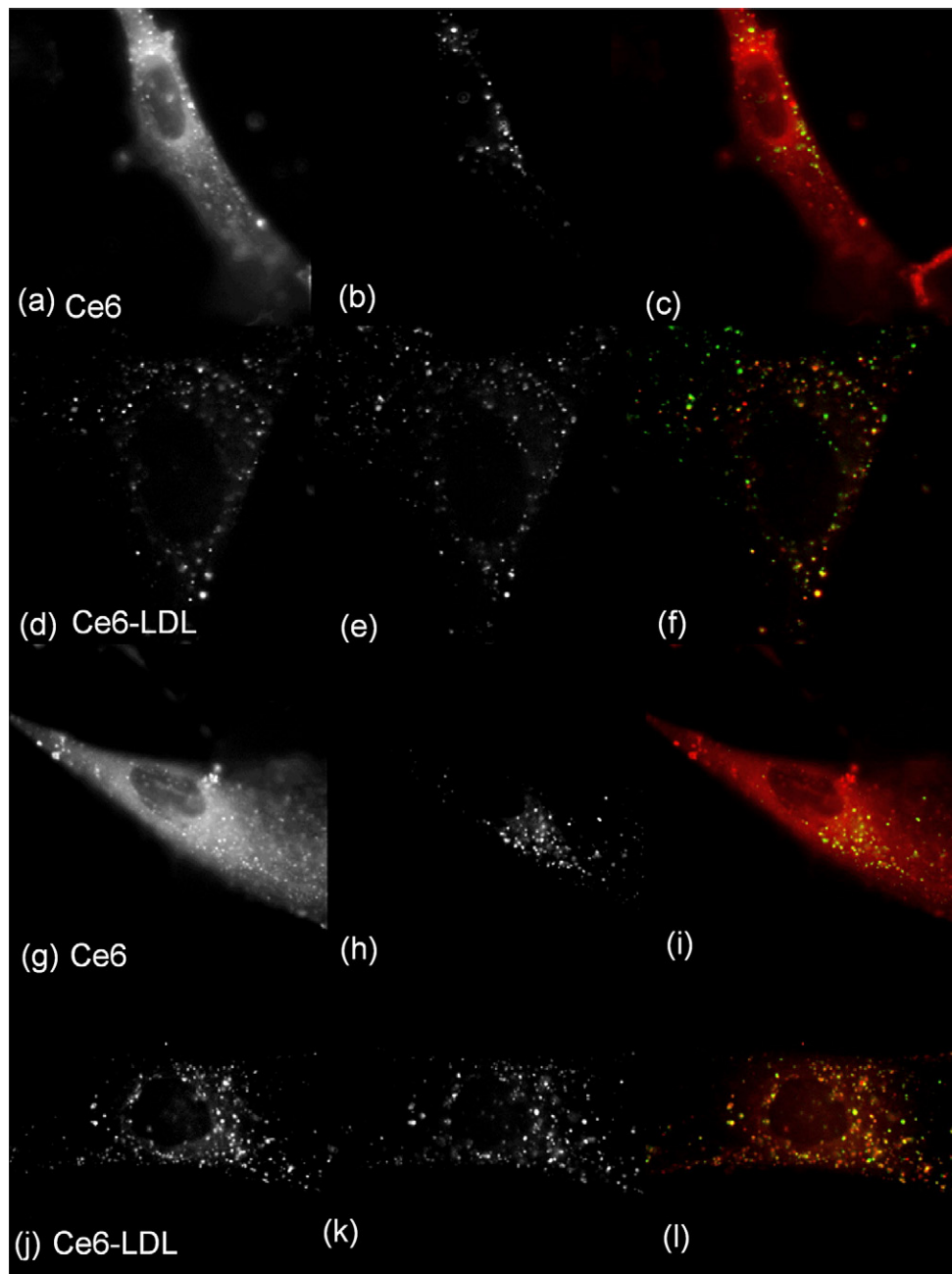


Fig. 7. Fluorescence microscopy study of the Ce6 cellular internalization by HS68 fibroblasts. First column (a, d, g, j) represents the Ce6 fluorescence emission, second column (b, e, h, k) represents the LysoTracker® green labeling and the last column (c, f, i, l) contains superposition of the red and green images. Yellow to orange spots represents the Ce6 localization in the lysosomes. (a, b, c) Cells incubated with [Ce6]=1.0 μM, pH=7.4. (d, e, f) Cells incubated with [Ce6]=1.0 μM, [LDL]=0.1 μM, pH=7.4. (g, h, i) Cells incubated with [Ce6]=1.0 μM, pH=6.9. (j, k, l) Cells incubated with [Ce6]=1.0 μM, [LDL]=0.1 μM, pH=6.9.

3.2.2. Subcellular localization

The cellular internalization pathway and the effect of LDL on the subcellular distribution of Ce6 were investigated by fluorescence microscopy. Fig. 7 shows that Ce6 is localized in the plasma membrane and in intracellular vesicles. In order to identify the nature of these vesicles, the lysosome-specific probe Lyso Tracker® green was used in co-localization experiments. Fig. 7 shows the fluorescence images of the cellular distribution of Ce6 (column 1), that of Lyso-Tracker® Green (column 2) and the resulting superposed image (column 3) at pH 7.4 and 6.9. In the absence of LDL, Ce6 labels the plasma membrane and intracellular vesicles (Figs. 7a, g). The overlap with the Lyso-Tracker Green image shows that only few vesicles are labeled by both Ce6 and Lyso-Tracker (Figs. 7c, i).

When Ce6 is vectorized by LDL the subcellular localization is different (Figs. 7d, j). The plasma membrane labeling is no more visible and Ce6 is mainly located in intracellular vesicles. The overlap of the red and green images indicates an enhanced co-localization (Figs. 7f, l). No significant effect of pH on subcellular distribution is observed.

4. Discussion

4.1. Kinetics of incorporation of Ce6 into liposomes

The extrusion technique is a suitable method producing vesicles that are sufficiently stable to resist the strong shear forces in fast mixing experiments. In all preliminary studies carried out by our group, we find no evidence for diameter changes or fusion of the extruded vesicles after they were mixed in the stopped-flow apparatus. Moreover, in the present study (see below) and a previous one [19] the binding constants derived from kinetics data and steady state experiments were identical within experimental errors confirming that the vesicles were in a similar state. The kinetics experiments described in the present work complement the steady state data reported previously [7]. In keeping with the structural similitude between dicarboxylic porphyrins and Ce6, we assumed that the incorporation of the chlorin proceeds in two steps. In the first step, the molecules incorporate into the outer membrane layer with their macrocycle buried into the lipid core and the charged lateral chains oriented to the water interface [21]. The second phase corresponds to a deeper incorporation into the hydrophobic core of the membrane and to the redistribution of the molecules between the two membrane hemileaflets. Depending on the structure of the photosensitizer and membrane properties, this phase can be relatively fast (deuteroporphyrin) or might last for hours (AlPcS_{2a}) [18].

The kinetic study of Ce6 interactions with the DOPC liposomes has shown that the first phase of the incorporation is extremely fast. The rate constants for the entrance and exist steps are $k_{\text{on}}^{\text{obs}} = (6.88 \pm 0.28) \times 10^5 \text{ M}^{-1} \text{ s}^{-1}$ and $k_{\text{off}}^{\text{obs}} = 125 \pm 12 \text{ s}^{-1}$ at pH 7.4 and $k_{\text{on}}^{\text{obs}} = (5.56 \pm 0.12) \times 10^5 \text{ M}^{-1} \text{ s}^{-1}$ and $k_{\text{off}}^{\text{obs}} = 58 \pm 4 \text{ s}^{-1}$ at pH 6.5. As reported for deuteroporphyrin [22], the entrance rate constant, $k_{\text{on}}^{\text{obs}}$, does not significantly depend on pH in this range. The value for Ce6 is somewhat lower than that for deuteroporphyrin, $1.69 \times 10^6 \text{ M}^{-1} \text{ s}^{-1}$

[22], which might be explained by the extra negative charge of the chlorine molecule. The second phase was not observable using DOPC liposomes. According to previous studies from our group, the rate of the transfer between two membrane leaflets, depends, among other factors, on the pH, on the temperature and on the hydrophobic barrier formed by the lipid hydrocarbon chains [21,23]. In order to facilitate the Ce6 transfer, we used DMOPC vesicles with shorter hydrocarbon chains. As in the case of DOPC, the melting temperature of DMOPC is far below zero. In both cases the bilayer is in a fluid phase. We also increased the temperature up to 37 °C. Under these conditions, the flip-flop was relatively slow at pH 7.4 ($t_{1/2} \sim 500 \text{ s}$) but it was significantly accelerated at pH 6.5 ($t_{1/2} \sim 40 \text{ s}$).

These results indicate that at pH 7.4, Ce6 populates rapidly the outer hemileaflet and then crosses the lipid bilayer very slowly. It can be noted that the rate of flip-flop of membrane lipids is significantly lower than the one for chlorin e6. However, phospholipids, chlorin e6 or other carboxylic photosensitizers such as deuteroporphyrin and AlPcS_{2a} significantly differ by their polar heads. Chlorin e6 is a good example illustrating an intermediate behavior between deuteroporphyrin and AlPcS_{2a}. Due to its three carboxylic groups and relatively short lateral chains (compared to DP), the PS' macrocycle localizes near the membrane surface and the flip-flop rate is considerably reduced compared to deuteroporphyrin. In fact, the flip-flop was observed at pH 7.4 only for bilayers made of C14 phospholipids and not observable over hours for more biological relevant C18 phospholipids. A lower pH favors the neutralization of the carboxylic groups and the macrocycle can locate deeper into the membrane and cross the bilayer. It must be kept in mind that the pK of carboxylic chains of deuteroporphyrin (and most likely those of chlorin e6) are significantly shifted to higher values when this molecule is incorporated within the bilayer as compared to the aqueous values. In fact, the apparent pKs of deuteroporphyrin in egg phosphatidylcholine are around 7.3 [24]. On the other hand, the non-neutralizable sulfonate groups in AlPcS_{2a} impede its transfer through the membrane.

If we take into account the observed monoexponential kinetics, the global binding constant can be defined as $K_B = k_{\text{on}}/k_{\text{off}}$. The values calculated, $5.5 \times 10^3 \text{ M}^{-1}$ for pH 7.4 and $9.6 \times 10^3 \text{ M}^{-1}$ for pH 6.5, are in good agreement with $K_{\text{DOPC}} = (5.9 \pm 1.1) \times 10^3 \text{ M}^{-1}$ for pH 7.4 and $K_{\text{DOPC}} = (9.1 \pm 0.6) \times 10^3 \text{ M}^{-1}$ for pH 6.5 previously determined by steady state experiments [7]. It should be noted, that in both static and dynamic experiments, the value of binding constants are referred to the total lipid concentration although only the outer membrane leaflet is populated.

4.2. Cellular experiments

Targeting of LDL-bound photosensitizers to neoplastic cells is one of the important mechanisms of their specific accumulation in proliferative tissues that over-express LDL-receptors [10,25–27]. Incorporation of the drugs by specific LDL-receptor mediated pathway drives them via the endocytosis compartment to lysosomes. Schmidt-Erfurth et al. have

studied the cellular uptake of free Ce6 and Ce6 covalently bound to LDL on fibroblasts and retinoblastoma cells [28]. Covalent binding to LDL significantly increased the uptake of Ce6 in both cell lines. Saturability and competitive inhibition studies indicated a receptor-mediated uptake. Binding at 2 °C also occurred, indicating a degree of non-specific associations. In our work, Ce6 is bound to LDL only by non-covalent interactions. Our system reflects the physiological conditions. Our results take into account the possibility of dynamic exchanges between all the plasmatic proteins as well as with the plasmic membrane. This was obviously not feasible with Ce6 conjugates. The goal of our work was not to target the Ce6 into cells but to understand the natural mechanisms of its selective retention by cancer cells. Despite evidence for the important role of the LDL-receptor mediated pathway, the importance of the LDL route *in vivo* has been questioned. Indeed, the tumor localizing ability is not always correlated with the photosensitizer's affinity for LDL [29]. In fact, great attention should be paid to the balance between the various cellular uptake processes, which depends on experimental conditions as outlined below.

In the present study, we have examined the cellular uptake and the subcellular localization of Ce6 either free in solution or preloaded to LDL. The amount of Ce6 associated (not covalently bound) to LDL is governed by equilibrium and dynamic constants. The objective was to establish the relative importance of passive diffusion, bulk endocytosis and LDL-mediated endocytosis on the uptake of the photosensitizer and on its subcellular distribution. As outlined in a previous paper, the partition of Ce6 among plasma proteins and lipid membranes depends on the ionization state of chlorin carboxylic chains [7]. Hence, a particular attention is given to pH effects.

4.2.1. Chlorin e6 cellular uptake

In agreement with Cunderlikova et al. [30], quantitative measurements revealed that the overall cellular uptake of Ce6 is increased upon decreasing pH (see Fig. 6). The enhanced drug uptake at pH 6.9 can be explained by the increased affinity of Ce6 toward lipid membrane at lower pH [7]. In the same way, the higher affinity of LDL for Ce6 at lower pH [7], explains that the uptake of Ce6 at pH 6.9 is higher than at pH 7.4. The ratio of intracellular Ce6 concentrations at pH 6.9 to that at 7.4 is approximately 1.3 for free and 1.9 for LDL-vectorized Ce6. These values are similar to the values of the ratio between the DOPC and LDL affinity constants determined at pH 6.5 and 7.4, which are 1.5 and 1.9 for DOPC and LDL respectively [7]. However, when the absolute values expressed as a function of protein content are considered, the situation appears more complex. Fig. 6 shows, that in our experimental conditions, the global cellular uptake of Ce6 is diminished when the drug is bound to LDL. In fact, two opposite effects should be considered. Firstly, the plasma membrane and LDL compete for Ce6 binding. Secondly, cells may take up LDL-bound Ce6 via LDL-mediated endocytosis. The positive or negative effect of the presence of LDL on Ce6 uptake depends on its relative affinity for LDL and plasma membrane, on the concentration of LDL and also on the level of expression of LDL receptors. The

importance of the last parameter is well exemplified in Fig. 5. Cells grown in a medium supplemented with Ultrosor G, favoring the expression of LDL receptors, incorporate significantly more Ce6. It is noteworthy that this medium has no effect on the uptake of free Ce6.

It must be pointed out that for *in vivo* conditions Ce6 does not exist as a free molecule because it is bound to blood carriers, namely albumin, HDL and LDL. From a dynamic point of view, the interactions between Ce6 and LDL or membranes are expected to be very fast. Experiments in solution have shown that the entrance and exit from LDL or albumin of amphiphilic photosensitizers take place within milliseconds [19,31]. Interactions with membranes are also extremely fast as reported above. No specific mechanism of cellular uptake of HSA or HDL bound photosensitizers has been reported so far. Thus, for *in vivo* conditions, even if the fraction of Ce6 bound to LDL is low, LDL-mediated endocytosis is likely to play a crucial role in its internalization pathway. Moreover, the supply of new LDL to the tumor stroma may lead to further Ce6 uptake. Indeed, as the dynamic of exchange is fast, naive LDL could extract Ce6 from other carriers.

The distribution of Ce6 among various carriers can be also modified by pH change. We previously showed [7] that a decrease of pH from 7.4 to 6.5 increases the affinity of Ce6 for LDL while its affinity for HSA is decreased. Ultracentrifugation studies led to the same conclusion [32]. As discussed in a previous paper, the distribution of Ce6 among its various carriers is likely to be shifted towards LDL at acidic pH. Indeed, different studies have shown that the pH of the interstitial fluid in tumors is lower than that in the normal tissues [8,9]. Both the overexpression of LDL receptors by neoplastic cells and this pH effect are likely to contribute to selective retention of amphiphilic carboxylic photosensitizers by tumors.

4.2.2. Subcellular localization

The subcellular distribution of Ce6 in absence or presence of LDL fully supports the above analysis. After 15 min incubation of HS68 fibroblasts with free Ce6 at pH 7.4, the fluorescence images revealed the presence of chlorin molecules in the plasma membrane and in intracellular vesicles. No labeling of the nucleus or cytosolic structures was found. This cellular distribution reflects the dynamics of the Ce6-membrane interactions as evidenced by the kinetics experiments on liposomes. In a first step, due to the lipophilicity of its macrocycle, Ce6 incorporates into the plasma membrane. It is worth noting that plasma membrane binding of other amphiphilic photosensitizers has been evidenced by total internal reflection fluorescence spectroscopy [33]. In agreement with the kinetics experiments, the passive diffusion of Ce6 through the membrane is extremely slow and the Ce6 incorporated in the plasma membrane is rather internalized in vesicular structures by absorptive endocytosis. The superposition of the red and green fluorescence emission of the LysoTracker® revealed only little Ce6 localization in the lysosomes (see Figs. 7a, b, c).

When the cells were incubated with Ce6-preloaded LDL, the chlorin was found to be localized mainly in intracellular vesicles (see Figs. 7d, e, f). The plasma membrane was not labeled. These results indicate that the balance between binding of Ce6

to membranes and LDL is shifted towards LDL favoring the drug uptake via the apo B/E receptor specific endocytosis. As a matter of fact, the overlap between Ce6 and LysoTracker® fluorescence shows that a main part of the photosensitizer is localized in lysosomes. Similar results were obtained with aluminum disulfonated phthalocyanine [18], a molecule also known for its inability to cross lipid bilayers [34].

As shown in Figs. 7g–l, pH decrease did not significantly modify the sub-cellular localization of Ce6 either free or associated to LDL. Little evidence for Ce6 internalization via passive diffusion was observed in agreement with the results on membrane models showing that a lipid bilayer with a biologically relevant thickness constitutes an efficient barrier even at the lower pH.

5. Conclusion

The present results provide new data to better understand the relationship between the structural parameters of photosensitizers and the dynamics of their interactions with membranes and lipoproteins. Together with results on porphyrins and phthalocyanines, these data can be further extrapolated to predict the impact of these interactions on the internalization pathway and subcellular distribution of these drugs.

The subcellular distribution of photosensitizers is a major determinant of their biological efficacy. Localization in the plasma membrane, mitochondria, endoplasmic reticulum and Golgi apparatus ensure the more efficient photoinduced cell death and the destruction of pathologic tissue in the context of photodynamic therapy [35,36]. On the other hand, the endosome/lysosomal localization of Ce6 can be further exploited in a new technology — photochemical internalization (PCI) [37]. In this approach the photochemical reactions break up the endosome/lysosome membrane and facilitate the liberation of drugs internalized by endocytosis. This technology has found applications *in vitro* as well as *in vivo*. The present results show that attention should be paid to the role of LDL as determinants of the subcellular localization, especially *in vivo*. Although, other mechanisms may come into play and/or other tumor compartments may be also involved, these data support the LDL route as an important selectivity factor.

Acknowledgments

Fluorescence microscopy experiments were performed by using the apparatus installed at CEMIM, a division of the National Museum of Natural History (MNHN) under the guidance of Dr. Marc Gèze and Dr. Marc Dellinger. We particularly thank Josiane Haigle for her skillful help in cellular experiments and Dr. Marc Gèze for his help in microscopy experiments. The stopped-flow apparatus was acquired thanks to subsidy from the charity associations ARC (grant #7209).

References

- [1] J.G. Levy, Photodynamic therapy, *Trends Biotechnol.* 13 (1995) 14–18.
- [2] T.J. Dougherty, Photodynamic therapy, *Adv. Exp. Med. Biol.* 193 (1985) 313–328.
- [3] J. Piette, C. Volanti, A. Vantieghem, J.Y. Matroule, Y. Habraken, P. Agostinis, Cell death and growth arrest in response to photodynamic therapy with membrane-bound photosensitizers, *Biochem. Pharmacol.* 66 (2003) 1651–1659.
- [4] D. Kessel, Y. Luo, Y. Deng, C.K. Chang, The role of subcellular localization in initiation of apoptosis by photodynamic therapy, *Photochem. Photobiol.* 65 (1997) 422–426.
- [5] A. Orenstein, G. Kostenich, L. Roitman, Y. Shechtman, Y. Kopolovic, B. Ehrenberg, Z. Malik, A comparative study of tissue distribution and photodynamic therapy selectivity of chlorin e6, Photofrin II and ALA-induced protoporphyrin IX in a colon carcinoma model, *Br. J. Cancer* 73 (1996) 937–944.
- [6] B. Pegaz, E. Debefve, F. Borle, J.P. Ballini, G. Wagnieres, S. Spaniol, V. Albrecht, D. Scheglmann, N.E. Nifantiev, H. van den Bergh, Y.N. Konan, Preclinical evaluation of a novel water-soluble chlorin E6 derivative (BLC 1010) as photosensitizer for the closure of the neovessels, *Photochem. Photobiol.* 81 (2005) 1505–1510.
- [7] H. Mojzisova, S. Bonneau, C. Vever-Bizet, D. Brault, The pH-dependent distribution of the photosensitizer chlorin e6 among plasma proteins and membranes: a physico-chemical approach, *Biochim. Biophys. Acta* 1768 (2007) 366–374.
- [8] L.E. Gerweck, K. Seetharaman, Cellular pH gradient in tumor versus normal tissue: potential exploitation for the treatment of cancer, *Cancer Res.* 56 (1996) 1194–1198.
- [9] J.L. Wike-Hooley, J. Haveman, H.S. Reinhold, The relevance of tumour pH to the treatment of malignant disease, *Radiother. Oncol.* 2 (1984) 343–366.
- [10] D. Kessel, Porphyrin–lipoprotein association as a factor in porphyrin localization, *Cancer Lett.* 33 (1986) 183–188.
- [11] G. Jori, M. Beltrami, E. Reddi, B. Salvato, A. Pagnan, L. Ziron, L. Tomio, T. Tsanov, Evidence for a major role of plasma lipoproteins as hematoporphyrin carriers *in vivo*, *Cancer Lett.* 24 (1984) 291–297.
- [12] J.P. Reyftmann, P. Morliere, S. Goldstein, R. Santus, L. Dubertret, D. Lagrange, Interaction of human serum low density lipoproteins with porphyrins: a spectroscopic and photochemical study, *Photochem. Photobiol.* 40 (1984) 721–729.
- [13] P.C. de Smidt, A.J. Versluis, T.J. van Berkel, Properties of incorporation, redistribution, and integrity of porphyrin–low-density lipoprotein complexes, *Biochemistry* 32 (1993) 2916–2922.
- [14] D. Gal, M. Ohashi, P.C. MacDonald, H.J. Buchsbaum, E.R. Simpson, Low-density lipoprotein as a potential vehicle for chemotherapeutic agents and radionuclides in the management of gynecologic neoplasms, *Am. J. Obstet. Gynecol.* 139 (1981) 877–885.
- [15] Y.K. Ho, R.G. Smith, M.S. Brown, J.L. Goldstein, Low-density lipoprotein (LDL) receptor activity in human acute myelogenous leukemia cells, *Blood* 52 (1978) 1099–1114.
- [16] O.H. Lowry, N.J. Rosebrough, A.L. Farr, R.J. Randall, Protein measurement with the Folin phenol reagent, *J. Biol. Chem.* 193 (1951) 265–275.
- [17] J.C. Maziere, C. Maziere, S. Emami, B. Noel, Y. Poumay, M.F. Ronveaux, E. Chastre, H. Porte, V. Barbu, S. Biade, Processing and characterization of the low density lipoprotein receptor in the human colonic carcinoma cell subclone HT29-18: a potential pathway for delivering therapeutic drugs and genes, *Biosci. Rep.* 12 (1992) 483–494.
- [18] S. Bonneau, P. Morliere, D. Brault, Dynamics of interactions of photosensitizers with lipoproteins and membrane-models: correlation with cellular incorporation and subcellular distribution, *Biochem. Pharmacol.* 68 (2004) 1443–1452.
- [19] K. Kuzelova, D. Brault, Kinetic and equilibrium studies of porphyrin interactions with unilamellar lipidic vesicles, *Biochemistry* 33 (1994) 9447–9459.
- [20] J.L. Goldstein, M.S. Brown, Binding and degradation of low density lipoproteins by cultured human fibroblasts. Comparison of cells from a normal subject and from a patient with homozygous familial hypercholesterolemia, *J. Biol. Chem.* 249 (1974) 5153–5162.
- [21] K. Kuzelova, D. Brault, Interactions of dicarboxylic porphyrins with unilamellar lipidic vesicles: drastic effects of pH and cholesterol on kinetics, *Biochemistry* 34 (1995) 11245–11255.

- [22] S. Bonneau, N. Maman, D. Brault, Dynamics of pH-dependent self-association and membrane binding of a dicarboxylic porphyrin: a study with small unilamellar vesicles, *Biochim. Biophys. Acta* 1661 (2004) 87–96.
- [23] N. Maman, D. Brault, Kinetics of the interactions of a dicarboxylic porphyrin with unilamellar lipidic vesicles: interplay between bilayer thickness and pH in rate control, *Biochim. Biophys. Acta* 1414 (1998) 31–42.
- [24] D. Brault, C. Vever-Bizet, T. Le Doan, Spectrofluorimetric study of porphyrin incorporation into membrane models—evidence for pH effects, *Biochim. Biophys. Acta* 857 (1986) 238–250.
- [25] G. Jori, E. Reddi, The role of lipoproteins in the delivery of tumour-targeting photosensitizers, *Int. J. Biochem.* 25 (1993) 1369–1375.
- [26] G. Jori, In vivo transport and pharmacokinetic behavior of tumour photosensitizers, *Ciba Found. Symp.* 146 (1989) 78–86 (discussion 86–94).
- [27] C.N. Zhou, C. Milanesi, G. Jori, An ultrastructural comparative evaluation of tumors photosensitized by porphyrins administered in aqueous solution, bound to liposomes or to lipoproteins, *Photochem. Photobiol.* 48 (1988) 487–492.
- [28] U. Schmidt-Erfurth, H. Diddens, R. Birngruber, T. Hasan, Photodynamic targeting of human retinoblastoma cells using covalent low-density lipoprotein conjugates, *Br. J. Cancer* 75 (1997) 54–61.
- [29] M. Kongshaug, J. Moan, S.B. Brown, The distribution of porphyrins with different tumour localising ability among human plasma proteins, *Br. J. Cancer* 59 (1989) 184–188.
- [30] B. Cunderlikova, L. Gangeskar, J. Moan, Acid–base properties of chlorin e6: relation to cellular uptake, *J. Photochem. Photobiol., B Biol.* 53 (1999) 81–90.
- [31] S. Bonneau, C. Vever-Bizet, P. Morliere, J.C. Maziere, D. Brault, Equilibrium and kinetic studies of the interactions of a porphyrin with low-density lipoproteins, *Biophys. J.* 83 (2002) 3470–3481.
- [32] B. Cunderlikova, M. Kongshaug, L. Gangeskar, J. Moan, Increased binding of chlorin e(6) to lipoproteins at low pH values, *Int. J. Biochem. Cell Biol.* 32 (2000) 759–768.
- [33] R. Sailer, W.S. Strauss, H. Emmert, K. Stock, R. Steiner, H. Schneck-enburger, Plasma membrane associated location of sulfonated meso-tetraphenylporphyrins of different hydrophilicity probed by total internal reflection fluorescence spectroscopy, *Photochem. Photobiol.* 71 (2000) 460–465.
- [34] N. Maman, S. Dhami, D. Phillips, D. Brault, Kinetic and equilibrium studies of incorporation of di-sulfonated aluminum phthalocyanine into unilamellar vesicles, *Biochim. Biophys. Acta* 1420 (1999) 168–178.
- [35] R.D. Almeida, B.J. Manadas, A.P. Carvalho, C.B. Duarte, Intracellular signaling mechanisms in photodynamic therapy, *Biochim. Biophys. Acta* 1704 (2004) 59–86.
- [36] N.L. Oleinick, R.L. Morris, I. Belichenko, The role of apoptosis in response to photodynamic therapy: what, where, why, and how, *Photochem. Photobiol. Sci.* 1 (2002) 1–21.
- [37] K. Berg, L. Prasmickaite, P.K. Selbo, M. Hellum, A. Bonsted, A. Hogset, Photochemical internalization (PCI)—a novel technology for release of macromolecules from endocytic vesicles, *Oftalmologia* 56 (2003) 67–71.